

## Diel vertical migration of the deep-water jellyfish *Periphylla periphylla* simulated as individual responses to absolute light intensity

Nicolas Dupont,<sup>a,\*</sup> T. A. Klevjer,<sup>b</sup> S. Kaartvedt,<sup>b</sup> and D. L. Aksnes<sup>a</sup>

<sup>a</sup>Department of Biology, University of Bergen, Bergen, Norway

<sup>b</sup>Department of Biology, University of Oslo, Oslo, Norway

### Abstract

We evaluate the hypothesis that the vertical migration of *Periphylla periphylla* is governed by its sensitivity to light intensity. By applying an individual-based model where random walk is combined with assumed individual responses to light, we compare the predicted vertical distributions with acoustical observations. Important features of the observed *P. periphylla* distributions can be explained by a simple proximate light response where individual *P. periphylla* avoids light above a certain threshold but also has a preference for very low light intensities. In addition to accounting for the observed synchronous diel vertical migration phenomenon in *P. periphylla*, this simple mechanism also accounts for simultaneous asynchronous vertical migrations observed for part of the population.

*Periphylla periphylla* is a mesopelagic coronate scyphomedusae of the family Periphyllidae and is considered to be a deep-water species with a global distribution (Fosså 1992). This species is established in exceptionally high abundances in at least three Norwegian fjords (Sørnes et al. 2007), but mass occurrences have also been recently observed in several other fjords although not yet reported (J.-A. Sneli pers. comm.; C. Schander pers. comm.; K. Eiane pers. comm.). The most studied *P. periphylla* occurrence is that in Lurefjorden, (60°41.7'N, 5°08.5'E) (Fig. 1). This fjord covers a surface area of about 30 km<sup>2</sup> and has a narrow opening to the outside coastal waters (200 m) and a shallow sill (20 m) (Sørnes et al. 2007). This makes the fjord less prone to advective exchange than most other fjords, making it a very useful location to study biological and ecological aspects of *P. periphylla*, such as developmental biology (Jarms et al. 1999, 2002), metabolism and behavior (Youngbluth and Båmstedt 2001), trophic ecology and feeding behavior (Sötje et al. 2007; Sørnes et al. 2008), and vertical distribution and migration (Båmstedt et al. 2003; Kaartvedt et al. 2007; Sørnes et al. 2008). These reports demonstrated that individuals stay deep in daytime and enter shallower depth at night. Indeed, *P. periphylla* is believed to be negatively phototactic (Youngbluth and Båmstedt 2001), and light seems to have a lethal photodegradation effect on the porphyrin pigment of the jellyfish (Jarms et al. 2002).

Diel vertical migration (DVM) is a common phenomenon in both marine and freshwater zooplankton species (Lampert and Sommer 2007), and its existence can be explained from different perspectives. From the proximate viewpoint external factors such as light (Richards et al. 1996), temperature or oxygen are regarded as drivers for the vertical movement (Dawidowicz and Carsten 1992; Lampert and Sommer 2007; Rossberg and Wickham 2008). Vertical migration can also be understood in terms of ultimate factors, that is, those affecting lifetime survival

and production of offspring. In the case where the water column offers reduced predation risk with increasing depth and increased growth opportunities at shallower depths, a specific vertical migration pattern can be analyzed as trade-off between these opposing vertical gradients. Thus, maximization of fitness (Fiksen and Carlotti 1998; De Robertis 2002) is here considered the ultimate cause for evolution of vertical migration patterns. Because the gradients in predation risk and food distribution are closely connected to environmental variables such as light, the proximate and the ultimate approaches are complementary rather than opposing.

Ringelberg (1999) observed that from the time evolutionary forces such as predation became included in analyses of DVM almost 30 yr ago, most of the studies have focused on ultimate factors to analyze and model DVM and argues that studies of proximate factors can still deliver understanding of DVM behavior (Ringelberg 1999; Ringelberg and Van Gool 2003). Also, there is a need to develop proximate rules of vertical behavior for organisms drifting in three-dimensional hydrodynamic models (Fiksen et al. 2007). Here we investigate such proximate mechanisms in *P. periphylla*.

We hypothesize that the vertical migration patterns of *P. periphylla* can be simulated by individual random walk that is constrained by avoidance and preference for certain light intensities. Specifically, we compare acoustical observations for periods with different photoperiods and different daylight with results from an individual-based simulation model in order to see if assumptions about simple proximate light mediated behavior could account for the observations.

### Methods

*A model of light sensitivity*—Two features suggest that *P. periphylla* is sensitive to light. First, vertical distributions during day and night (Youngbluth and Båmstedt 2001; Båmstedt et al. 2003; Kaartvedt et al. 2007) suggest that *P.*

\* Corresponding author: nicolas.dupont@bio.uib.no

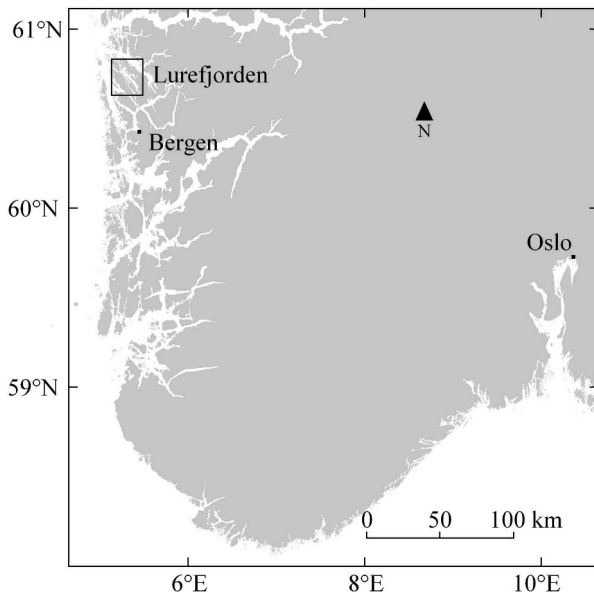


Fig. 1. The location of Lurefjorden on the west coast of Norway.

*periphylla* are located deeper in illuminated water. Second, *P. periphylla* has an organ, rhopalia (Jarms et al. 2002), that contains photoreceptor cells. We will assume that an individual can sense and swim vertically to regulate its ambient light. We further assume that an individual can, during the time step  $\Delta t$ , swim from depth  $Z_t$  to  $Z_{t+\Delta t}$ , where  $Z_{t+\Delta t} = Z_t + \Delta Z_{med}$  and where

$$\Delta Z_{med} = \alpha V \Delta t \quad (1)$$

Here,  $\alpha$  is a behavioral variable that takes the value of either 1 (movement towards higher light) or  $-1$  (movement towards less light), and  $V$  is the vertical swimming speed. Vertical movement of *P. periphylla* is constrained by the surface and the bottom. These boundaries are represented so that if Eq. 1 suggests a new location “below the bottom” or “over the surface,” the boundaries act as a mirror so that the individual is reversed to a position within the water column without changing the total distance swam ( $|\Delta Z_{med}|$ ) during the time step.

The ambient light,  $E_{med}$ , at depth  $Z_{med}$  was calculated from the surface irradiance,  $E_0$ , and the attenuation of downwelling irradiance  $K$  according to the Beer-Lambert law,  $E_{med} = E_0 \exp(-KZ_{med})$  (Fig. 2A) (see Table 1 for a summary of the symbols). The photoresponse of *P. periphylla* is unknown, and we therefore made different assumptions (C1–C3 below) for how  $\alpha$  is affected by the ambient light (Fig. 2B–D).

C1: According to a study of Jarms et al. (2002), *P. periphylla* avoids strong irradiance, and in the simplest case we assume that an individual avoids light above a certain fixed threshold,  $E_{max}$  (Fig. 2B) so that if  $E_{med} \geq E_{max}$ , then  $\alpha = -1$ , which means that the individual swims away from the light. If  $E_{med} < E_{max}$ , we assume that it will move toward (with probability  $p$ ) or away from (probability  $q$ ) the light source with equal probabilities (hereafter referred

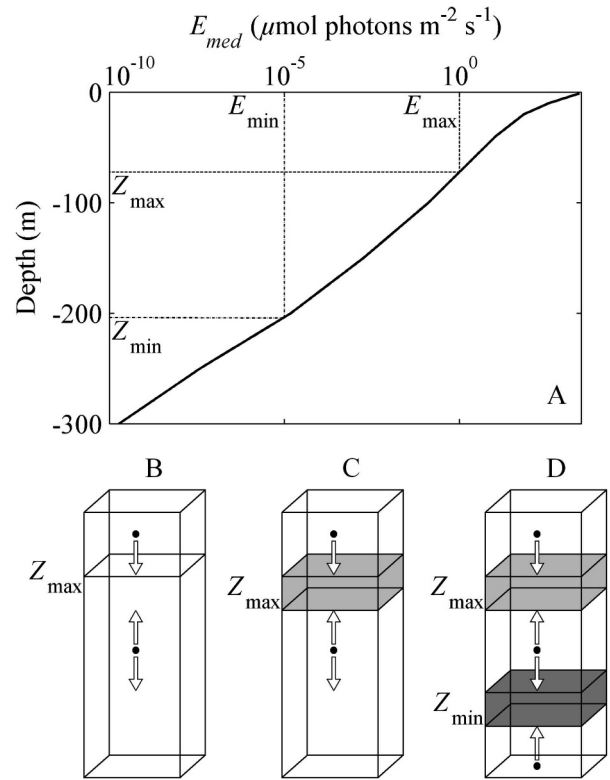


Fig. 2. Conceptual scheme of the model. (A) How  $Z_{max}$  and  $Z_{min}$  relate to  $E_{max}$  and  $E_{min}$  for a particular vertical  $E_{med}$  profile. (B) The simulated case, C1, where an individual avoid light stronger than a fixed  $E_{max}$ . (C) C2 with individual variation in  $E_{max}$ . (D) C3 with individual variations in  $E_{max}$  and  $E_{min}$ . The arrows represent the swimming directions (upward  $\alpha = 1$  or downward  $\alpha = -1$ ).

to as “free swimming”):

$$\begin{aligned} p &= P(\alpha = 1) = P(R \geq 0.5) \\ q &= P(\alpha = -1) = P(R < 0.5) \end{aligned} \quad (3)$$

where  $R$  is a uniform random number between 0 and 1.

C2: Here individuals have different tolerances for light; that is,  $E_{max}$  varies among individuals (Fig. 2C). Such variation (specified by  $\sigma_{E_{max}}^2$ ) might reflect different genotypes (Ringelberg 1999), size, hunger, or other individual states frequently represented in state-dependent simulation models (Giske et al. 1998).

C3: In addition to light avoidance as in C2, we now also introduce light preference so that an individual exposed to light below a threshold,  $E_{min}$ , swims toward stronger light; that is, if  $E_{med} \leq E_{min}$ , then  $\alpha = 1$  (Fig. 2D). As for  $E_{max}$  in C2,  $E_{min}$  also varies ( $\sigma_{E_{min}}^2$ ) among individuals. Free swimming ( $p = q = 0.5$ ) was assumed for an individual occupying a depth with ambient light within the two thresholds.

*Acoustical observations*—A 38-kHz SIMRAD EK60 echosounder was located on the seabed at  $\sim 270$ -m depth

Table 1. Explanation of the symbols used in the simulation model.

Symbol	Explanation	Unit
$E_{med}$	Light level at depth $Z_{med}$	$\mu\text{mol photons m}^{-2} \text{ s}^{-1}$
$K$	Attenuation of downwelling irradiance	$\text{m}^{-1}$
$Z_{med}$	Depth of an individual	m
$E_{max}$	Upper irradiance tolerance for jellyfishes	$\mu\text{mol photons m}^{-2} \text{ s}^{-1}$
$E_{min}$	Lower irradiance tolerance for jellyfishes	$\mu\text{mol photons m}^{-2} \text{ s}^{-1}$
$\sigma_{E_{max}}^2$	Variance of $E_{max}$	$\mu\text{mol photons}^2 \text{ m}^{-4} \text{ s}^{-2}$
$\sigma_{E_{min}}^2$	Variance of $E_{min}$	$\mu\text{mol photons}^2 \text{ m}^{-4} \text{ s}^{-2}$
$p$	Probability to move upward	Dimensionless
$q$	Probability to move downward	Dimensionless
$R$	Uniformly distributed variable	Dimensionless
$\Delta Z_{med}$	Distance done per time step	m
$\Delta t$	Time step	s
$V$	Vertical swimming speed	$\text{m s}^{-1}$
$\alpha$	Swimming direction coefficient	Dimensionless

in Lurefjorden in an upward-looking mode, scanning the water column once per second from January to April 2007. All acoustically detected single targets in the deep waters (>150 m) of Lurefjorden were assumed to originate from *P. periphylla* as previously described by Kaartvedt et al. (2007).

Both individual positions and biomass distribution of *P. periphylla* were assessed acoustically using, respectively,

target tracking of resolved individuals (*see* below) and echo integration of total backscatter. Depths <150 m at daytime were omitted from the echo integration, as *P. periphylla* echoes cannot be properly separated from echoes of other objects in an automatic quantitative analysis. The observed daytime vertical distribution of *P. periphylla* is therefore truncated. Indeed, immediately above an acoustic scattering layer of *P. periphylla* is a layer identified through trawling (Båmstedt et al. 2003) as being dominated by northern krill (*Meganyctiphanes norvegica*) and pelagic fishes associated with the krill layer. As krill and fish migrated toward the surface at night, the range for echo integration of *P. periphylla* increased, and integration from nighttime encompassed the whole water column, apart for the upper 14 m. To reduce the influence of the strong backscatter of fish on the relative biomass profiles, integration was performed twice, once with a threshold of  $-75$  dB, where fish will be the main contributor to the backscatter, and once at a threshold of  $-100$  dB, where the *P. periphylla* population will contribute to the backscatter. Relative densities were then computed from the difference of results between the  $-75$ - and the  $-100$ -dB threshold.

For comparisons with simulation results, we chose four dates for echo integration: 22 and 23 February 2007 and 07 and 08 April 2007. These were selected to reflect different photoperiods (February vs. April) and two consecutive days: one sunny with high incoming irradiance and one cloudy with low irradiance (Table 2).

Table 2. Surface irradiance measured at the Department of Geophysics, University of Bergen. We converted these observations from  $\text{J m}^{-2} \text{ h}^{-1}$  to  $\mu\text{mol photons m}^{-2} \text{ s}^{-1}$  according to the conversion factor  $1.3 \times 10^{-3}$  (Valiela 1995).

Hour	Date and condition				
	22 Feb 2007	23 Feb 2007	07 Apr 2007	08 Apr 2007	15 Apr 2007
	Sunny	Cloudy	Sunny	Cloudy	Sunny
1	—	—	—	—	—
2	—	—	—	—	—
3	—	—	—	—	—
4	—	—	—	—	—
5	—	—	12.8	12.8	64
6	—	—	64	76.8	384
7	12.8	—	140.8	179.2	985.7
8	294.4	51.2	320	243.2	1574.5
9	742.4	102.4	460.8	243.2	2112.1
10	1139.3	166.4	1075.3	268.8	2534.6
11	1254.5	204.8	2137.7	256	2803.4
12	1241.7	243.2	2432.2	281.6	2867.4
13	1152.1	192	1715.3	268.8	2790.6
14	588.8	217.6	1356.9	166.4	2560.2
15	422.4	102.4	1139.3	140.8	2188.9
16	140.8	76.8	896.1	128	1484.9
17	12.8	12.8	563.2	76.8	1036.9
18	—	—	320	38.4	435.2
19	—	—	12.8	—	64
20	—	—	—	—	—
21	—	—	—	—	—
22	—	—	—	—	—
23	—	—	—	—	—
24	—	—	—	—	—

**Target tracking of *P. periphylla***—The procedure of combining sequential echoes from the same target into so-called tracks is known as target tracking. In the current study, target tracking for analysis of individual swimming behavior was performed over the depth range from 270-m up to 150-m depth because tracks above this depth were considered unreliable at daytime. A target strength (TS) threshold of  $-70$  dB was applied to the echogram prior to single echo detection, and echoes were detected using the cross-filter detector of Sonar5 (Balk and Lindem 2005). This threshold implies a strong bias against weaker scatters, and consequently only a small proportion of the total echoes are detected using our settings, and the relative units we report on *P. periphylla* are biased toward the larger individuals.

Tracks were detected by an automated tracking algorithm that required tracks to have at least 20 registered echoes, with a maximal vertical excursion of 30 cm allowed between registered echoes in the tracks. Up to five consecutive missing registrations were allowed. With ping rates of  $\sim 1$  s $^{-1}$ , minimal track length was therefore approximately 20 s. Each detected track was divided into behavioral segments according to the three behavioral states: upward swimming, pause, and downward swimming. The boundaries between these states were set to  $\pm 0.5$  cm s $^{-1}$  (ping-to-ping vertical speeds smoothed with a 20-point running mean). If the state changed within a track, a new segment of that track was defined. A minimum of 10 echoes were demanded for each segment. Tracking was performed on data recorded in the period from 10 to 30 January 2007. From the results of tracking, we obtained frequency distributions of the duration of the period ( $T$ ) (Fig. 3A) for which an individual swam in the same direction and of swimming speed ( $V$ ) (Fig. 3B).

**Parameter values assumed in the simulations**—Hourly measurements of surface light was provided by the Department of Geophysics, University of Bergen (Table 2). Linear interpolation between hourly observations was used in the simulations. The measurements were insensitive to light variations at night, and we assumed a nocturnal surface irradiance of  $4.6 \times 10^{-4}$   $\mu\text{mol photons m}^{-2} \text{s}^{-1}$  (representing moonlight irradiance in Contor and Griffith 1995) for the lacking night observations of Table 2. Values of the attenuation of downwelling irradiance,  $K$ , were assumed from measurements in Lurefjorden in November 2006 (Aksnes et al. in press). Table 3 gives the assumed values of  $E_{\text{max}}$ ,  $E_{\text{min}}$ ,  $\sigma_{E_{\text{max}}}^2$ , and  $\sigma_{E_{\text{min}}}^2$  that were used in the simulations.

For each individual and each time step ( $\Delta t$ , Table 3), the swimming speed ( $V$ , Eq. 1) is randomly chosen from the exponential distribution that was fitted to the observed swimming speed distribution (Fig. 3B).

**Simulations**—Each simulation included three steps. First, the initial condition was established by distributing a certain number of individuals randomly in the water column. Second, during a spin-up period of 24 h, the individuals were allowed to redistribute according to the assumptions of the model, and the results obtained for the

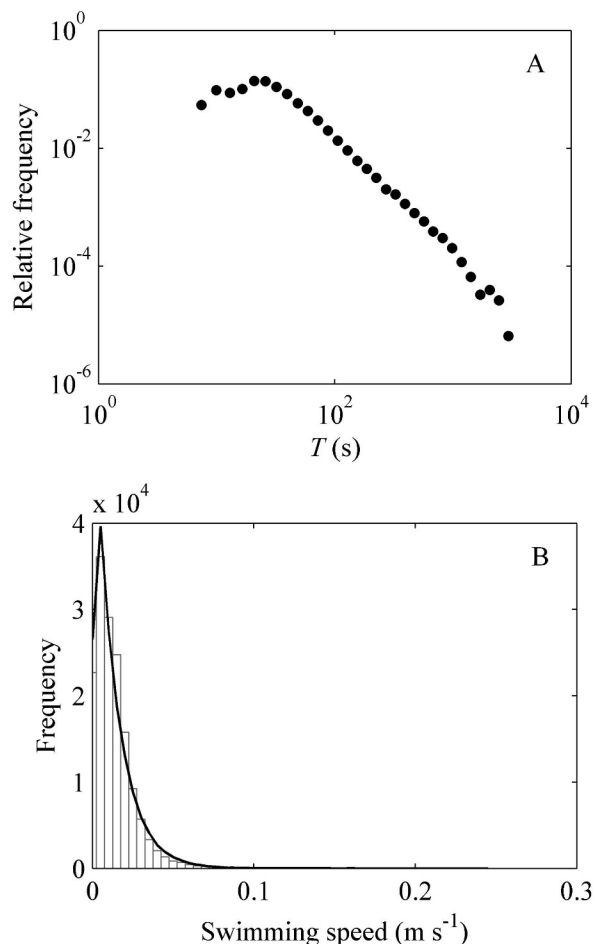


Fig. 3. (A) Observed relative frequency distributions of the duration of the period ( $T$ ) for which an individual swam in the same direction based on individual acoustical tracking of *P. periphylla* in Lurefjorden. (B) Exponential distribution (black line) fitted to the observed individual swimming speed ( $V$ ) distribution.

next 24-h period were compared with acoustical observations. Simulated ( $M_i$ ) and observed ( $D_i$ ) depths for the 80th percentile of the vertical distribution on 15 April 2007 are compared according to the model efficiency (ME) method

Table 3. Values of parameters used in the simulations. The time step,  $\Delta t$ , was set according to the median duration of the observed period ( $T$ ) for which an individual swam in the same direction (Fig. 3A).  $E_{\text{max}}$ ,  $E_{\text{min}}$ ,  $\sigma_{E_{\text{max}}}^2$ , and  $\sigma_{E_{\text{min}}}^2$  were approximated from the depth ranges reported for medusae larger than 4 cm in table 3 in Sørnes et al. (2007).

Parameters	Values	Unit
$\Delta t$	21.6	s
$E_{\text{max}}$	0.18	$\mu\text{mol photons m}^{-2} \text{s}^{-1}$
$E_{\text{min}}$	$2.6 \times 10^{-5}$	$\mu\text{mol photons m}^{-2} \text{s}^{-1}$
Minimum $\sigma_{E_{\text{max}}}^2$	$0.6 \times 10^{-2}$	$\mu\text{mol photons}^2 \text{m}^{-4} \text{s}^{-2}$
Maximum $\sigma_{E_{\text{max}}}^2$	$13.6 \times 10^{-2}$	$\mu\text{mol photons}^2 \text{m}^{-4} \text{s}^{-2}$
Minimum $\sigma_{E_{\text{min}}}^2$	$0.3 \times 10^{-8}$	$\mu\text{mol photons}^2 \text{m}^{-4} \text{s}^{-2}$
Maximum $\sigma_{E_{\text{min}}}^2$	$7.5 \times 10^{-8}$	$\mu\text{mol photons}^2 \text{m}^{-4} \text{s}^{-2}$

described in Allen et al. (2007):

$$ME = 1 - \frac{\sum_{i=1}^n (D_i - M_i)^2}{\sum_{i=1}^n (D_i - \bar{D})^2} \quad (4)$$

where  $\bar{D}$  is the mean of all  $D_i$ s.

## Results

**Simulated migration patterns**—Individual-based models (IBM) provide predictions at the population as well as at the individual level. The predicted individual migrations of C1 and C2 did not result in a detectable synchronous migration at the population level (Fig. 4A,B). The asynchronous swimming of C1 predicts that the major part of the population is located between 100 and 210 m with a median depth around 150 m during both day and night (Fig. 4A). Similarly, C2 results in a population that distributes between 125 and 250 m with a median depth of 180 m during both day and night (Fig. 4B). On the contrary, C3 predicts a synchronized DVM pattern that is clearly detectable at the population level (Fig. 4C). It should be noted, however, that some of the individuals in C3 does not show a distinct DVM (Fig. 4C).

**Acoustical observations at day and night**—Because of methodological constraints (see Methods), we lack acoustic estimates of jellyfish abundance above 13.75 m at nighttime and above 150 m at daytime (Fig. 5A). At night, *P. periphylla* is spread all over the water column. The abundance is low, below 150 m, with a distinct increase in abundance toward the surface at night. During daytime, the abundance below 150 m is up to three times higher than at nighttime (Fig. 5A). This suggests that the bulk of *P. periphylla* in waters below 150 m perform synchronous DVM, but a part of the population occurs in deep water also at night (Fig. 5A,B).

**Sensitivity of the migration patterns to individual variations in  $E_{max}$  and  $E_{min}$** —The predicted vertical distributions of the three different cases presented in Fig. 4 were compared with the observed *P. periphylla* distributions on 15 April 2007 by use of the ME method of Allen et al. (2007) (Table 4) by varying the individual variation in  $E_{max}$  and  $E_{min}$  (i.e., the values of  $\sigma_{E_{max}}^2$  and  $\sigma_{E_{min}}^2$ ). C3 had the highest score with a maximum ME value of 0.58, which corresponds to a very good fit on the scale of Allen et al. (2007).

In C3, the highest ME values are reached at high values of  $\sigma_{E_{max}}^2$  and low values of  $\sigma_{E_{min}}^2$  (Fig. 6). When  $\sigma_{E_{max}}^2$  and  $\sigma_{E_{min}}^2$  in C3 are at the minimum, a synchronous DVM appears (Fig. 7A). However, the simulated distribution is narrow and located 100 m above the observed daytime distribution. An increase of  $\sigma_{E_{max}}^2$  generally deepens and widens the vertical daytime distribution and provides the best fit to the observations (Fig. 7B). An increase of  $\sigma_{E_{min}}^2$  reduced the synchronous DVM (Fig. 7C). Here, the major part of the population is located below 75 m in both day

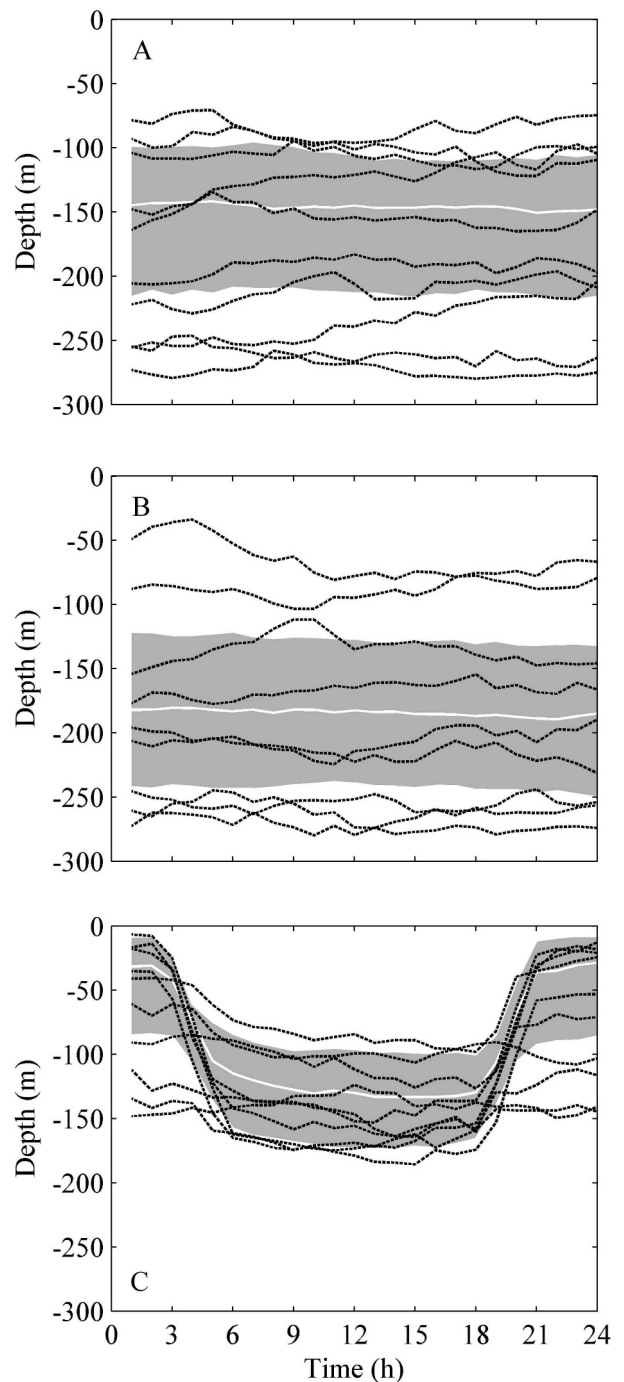


Fig. 4. The shaded areas represent the depth range occupied by 60% of 211 simulated individuals. The median depth is indicated by the white line. Individual tracks for 10 randomly selected individuals are indicated by the dashed lines. (A) C1 configuration. (B) C2 configuration. (C) C3 configuration.

and night, and a poor fit with observations appears. The effect of increasing both variances leads also to a slightly synchronous DVM visible only in the shallowest part of the distribution (Fig. 7D). It should be noted, however, that although notable synchronous migration is lacking in Fig. 7C,D, asynchronous migration occurred at the individual level as illustrated in Fig. 4A,B.

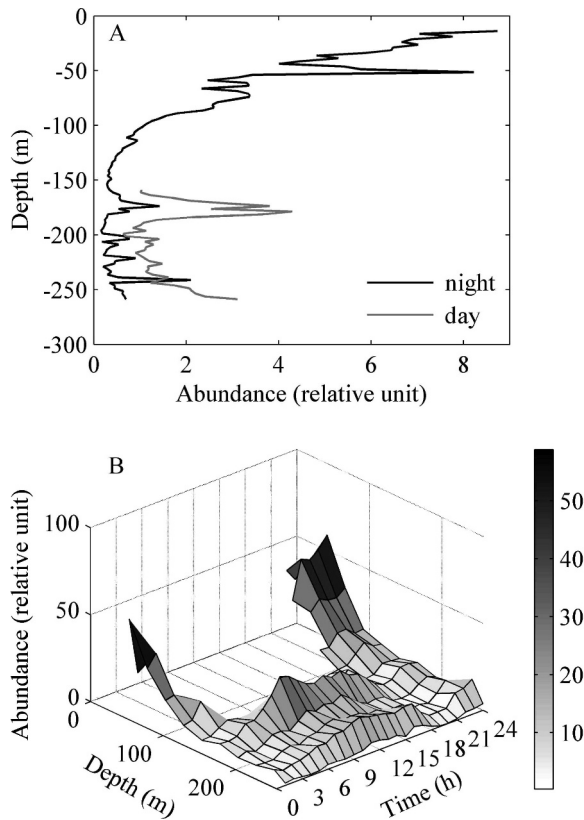


Fig. 5. (A) Vertical distribution of *P. periphylla* in Lurefjorden on 15 April 2007. Data obtained by acoustical integration every 1.5 m at midnight (bold line) and at noon (dashed line). (B) Three-dimensional plot of the abundance obtained with acoustics as a function of time and depth integrated every 25 m. The empty area represents lack of acoustical data above 150-m depth during day time.

*Differences between observed and simulated populations*—The simulated case that gave the best fit on 15 April 2007 (C3, Fig. 7B) where now applied with the same parameter values for the two periods 22–23 February 2007 (Fig. 8A,B) and 07–08 April 2007 (Fig. 8C,D). The simulations appear more consistent with the observations at nighttime than at daytime (Fig. 8). It should, however, be noted that observations are incomplete at daytime and that only the deepest part of the vertical distributions could be compared. At daytime, the location of the simulated deep 80th

Table 4. Values of the model efficiency (ME) method (Allen et al. 2007) for the three different configurations of the model (C1–C3; see Methods). The lowest and highest score are given for C2 and C3 on the basis of 441 different simulations (set of 21 different values for  $\sigma_{E_{\max}}^2$  and  $\sigma_{E_{\min}}^2$ ). The scores for ME are classified according to Allen et al. (2007), such as  $<0.2$  = a poor fit,  $0.2$ – $0.5$  = a good fit,  $0.5$ – $0.65$  = a very good fit, and  $>0.65$  = an excellent fit.

	C1	C2	C3
ME value	–3.99	–7.23 to –2.65	–5.84 to 0.58
Best fit	Poor	Poor	Very good

percentile is consistently located shallower than the observed (Fig. 8). The daytime deepening of the observed 80th percentile is explained by an increase in the relative abundance located below 150 m, from about 10% at nighttime to a maximum value of about 30% in February and 50% in April (Fig. 9).

A mismatch appears, both in the percentiles (Fig. 8) and in the relative abundances (Fig. 9), in the timing of the dawn (downward) and dusk (upward) synchronous migrations. The dawn mismatch is less in April (Fig. 8C,D) than in February (Fig. 8A,B), while the dusk mismatch is similar at all dates. Furthermore, before midnight the relative abundances deeper than 150 m increase at all dates, and this feature (often referred to as “midnight sinking”) is not reproduced by the model.

## Discussion

Based on acoustical observations of single individuals, Kaartvedt et al. (2007) found that the migratory behavior of *P. periphylla* could be classified as a mixture of synchronous DVM and asynchronous migration. Similar evidence has been provided in a study (Sötje et al. 2007) where individual behavior was observed with a remote-operated vehicle. They observed that the orientation of the individuals at dawn and dusk showed no consistency with synchronous DVM. From a theoretical point of view, different behavior is expected for individuals having different states, such as size, hunger level, maturation, and so on (Mangel and Clark 1988; Pearre 2003). Certain parameterizations of our simple simulation model did predict a mixture of synchronous and asynchronous migration patterns (Fig. 4C), and these results were actually caused by variation in individual state, that is, in individual variation in light sensitivity. Thus, our study suggests that a simple behavioral algorithm involving random walk within a preferred range of light intensities has the potential to simulate a mixture of synchronous and asynchronous vertical migration modes as reported by Kaartvedt et al. (2007).

A main result in our study is that no notable synchronous DVM were predicted in the simulations where only avoidance of light was assumed for *P. periphylla*. Notable synchronous DVM patterns (Fig. 4C) emerged only when we also introduced the assumption of preference for a low light intensity. While there is experimental evidence of light avoidance in *P. periphylla* (Jarms et al. 2002; Sötje et al. 2007), such evidence lacks concerning light preference. *P. periphylla* is regarded as a forager not relying on vision (Sørnes et al. 2008), so light preference should not be expected for that reason. However, light might be a proxy for other habitat characteristics of importance to *P. periphylla*, such as prey. Distributions of prey species, such as *Calanus* spp. (Sørnes et al. 2008) and *Meganyctiphanes norvegica*, are known to correlate with variation in light (Irigoien et al. 2004; Kaartvedt et al. 2007).

*Different hypotheses for the DVM phenomenon*—It is well known that migration in plankton organisms are affected by variation in light, and several hypotheses have been

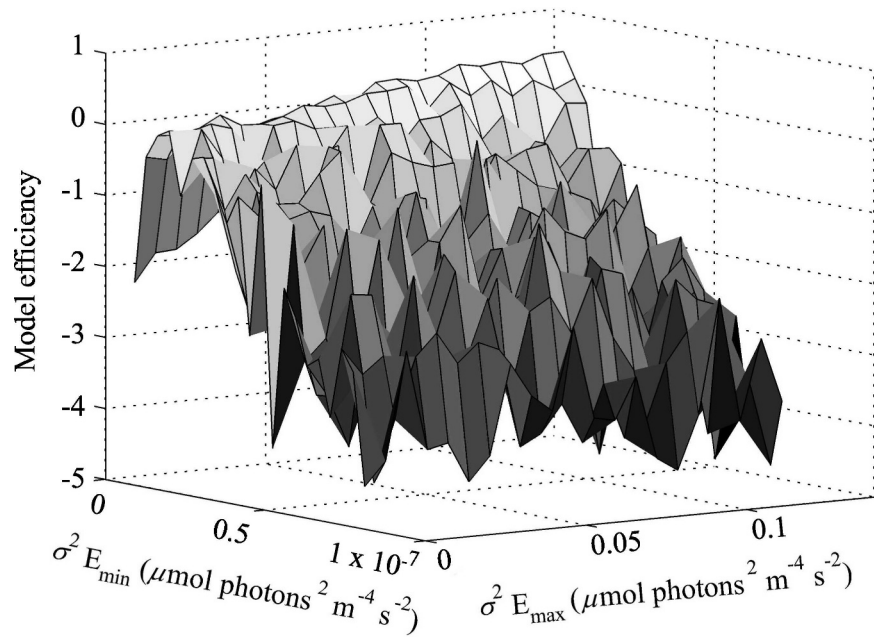


Fig. 6. Three-dimensional representation of the model efficiency (ME) method from 441 simulations as a function of  $\sigma_{E_{\max}}^2$  and  $\sigma_{E_{\min}}^2$  for C3.

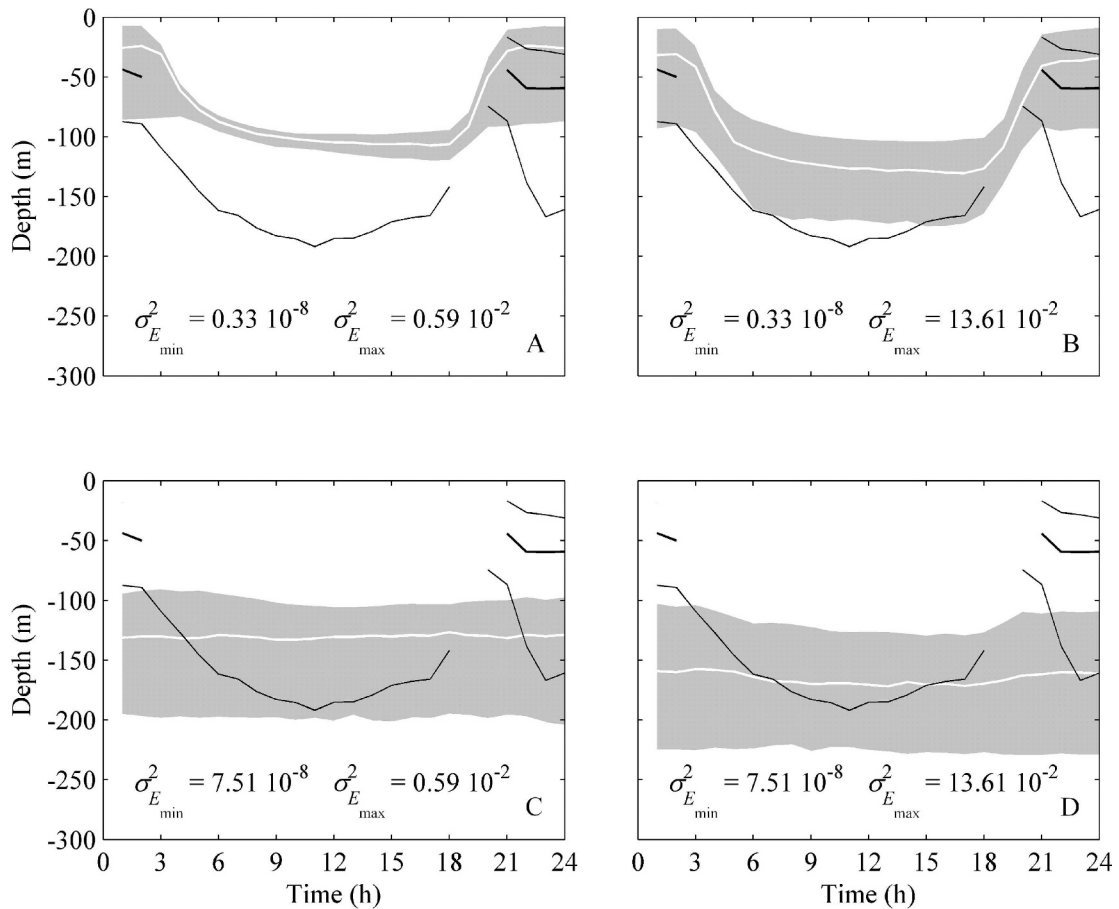


Fig. 7. Simulated and observed vertical distributions. The simulated distributions were derived from 211 simulated individuals (C3) with different values of  $\sigma_{E_{\max}}^2$  and  $\sigma_{E_{\min}}^2$  in  $\mu\text{mol photons}^2 \text{m}^{-4} \text{s}^{-1}$  as indicated. The shaded area represents the vertical location of 60% of the simulated individuals; that is, the borders represent the two 80th percentiles of the distribution. The median depth is indicated by the bold white line. Similarly, the thin black lines represent the two 80th percentiles of the observed distribution, while the median depth is indicated by the bold black line. Note that the observed shallow 80th percentile and median depth lack at daytime. The observations represent 15 April 2007, and the simulations were forced with the light measurements at this date.

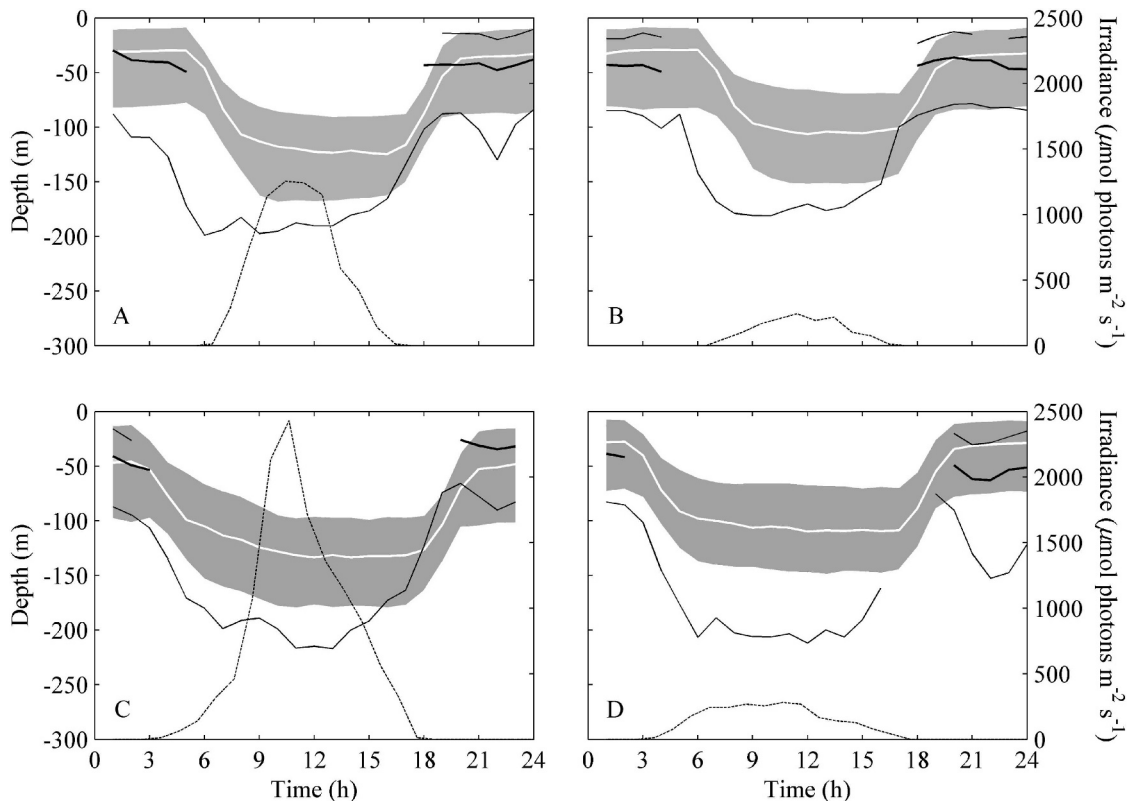


Fig. 8. Simulated (C3) and observed vertical distributions for (A) 22 February 2007, (B) 23 February 2007, (C) 07 April 2007, and (D) 08 April 2007, where  $\sigma_{E_{\max}}^2 = 13.61 \times 10^{-2}$  and  $\sigma_{E_{\min}}^2 = 0.33 \times 10^{-8} \mu\text{mol photons}^2 \text{m}^{-4} \text{s}^{-2}$ . The surface light intensity is indicated by the dashed line. See Fig. 7 for explanation of the shaded area and the other lines.

proposed to explain how migrations relate to such variation (Richards et al. 1996; Ringelberg 1999; Pearre 2003). First, it has been hypothesized that the zooplankton moves toward a preferred absolute light intensity, referred to as the preferred light intensity mechanism. Second, zooplankton moves vertically so that changes in the ambient light intensity were minimized (rate of change mechanism) and finally that zooplankton responds to the relative rate of change in light intensity (relative rate of change mechanism). Our proposed mechanism has some similarity with the preferred light intensity mechanisms. However, rather than swimming toward a specific absolute intensity, we assume that *P. periphylla* individuals swim constantly within a preferred range of absolute light intensity. The absolute light intensity hypothesis did not provide satisfactory fit with observations in previous modeling studies of DVM in zooplankton (Andersen and Nival 1991; Richards et al. 1996). It should be noted that these and other approaches have attempted to explain the observed synchronous migration speed (i.e., at the population level) as a direct function of observed changes in light intensity. In our study, we do not assume a particular relationship between the individual swimming speed and changes in light.

The IBM approach allows an explicit representation of mechanisms operating at the individual level, and the DVM can then be understood as an emergent property from variation in individual behavior. In our model, changing

light exposes individuals to suboptimal light levels, and the swimming direction, although not the speed, therefore changes from a random to a directional walk. This simple mechanism causes the simulated DVM where it appears as if the swimming speed is higher at dusk and dawn than during day and night. As demonstrated in our simulations, this does not imply that the population migration rate is independent of change in light, and in future studies it might be of interest to investigate more generally to what extent our proposed mechanisms can predict DVM that appears consistent with the light control hypotheses referred to previously.

*Inconsistencies between simulations and observations*—Not surprisingly, our simple model cannot account for several observed features of the migration patterns in *P. periphylla*. Simulations are not consistent with observations, notably at night, where some individuals are migrating downwards in a so-called midnight sinking for *P. periphylla* (Kaartvedt et al. 2007; see also Figs. 8A,D, 9). Furthermore, at dawn the observed population migrates downward before the simulated population (Figs. 8, 9), and during daytime the simulated 80th percentile is shallower than the observed (Fig. 8). These differences probably reflect inadequate assumptions about the behavior of *P. periphylla* in the model, but methodological inadequacies might also be responsible.

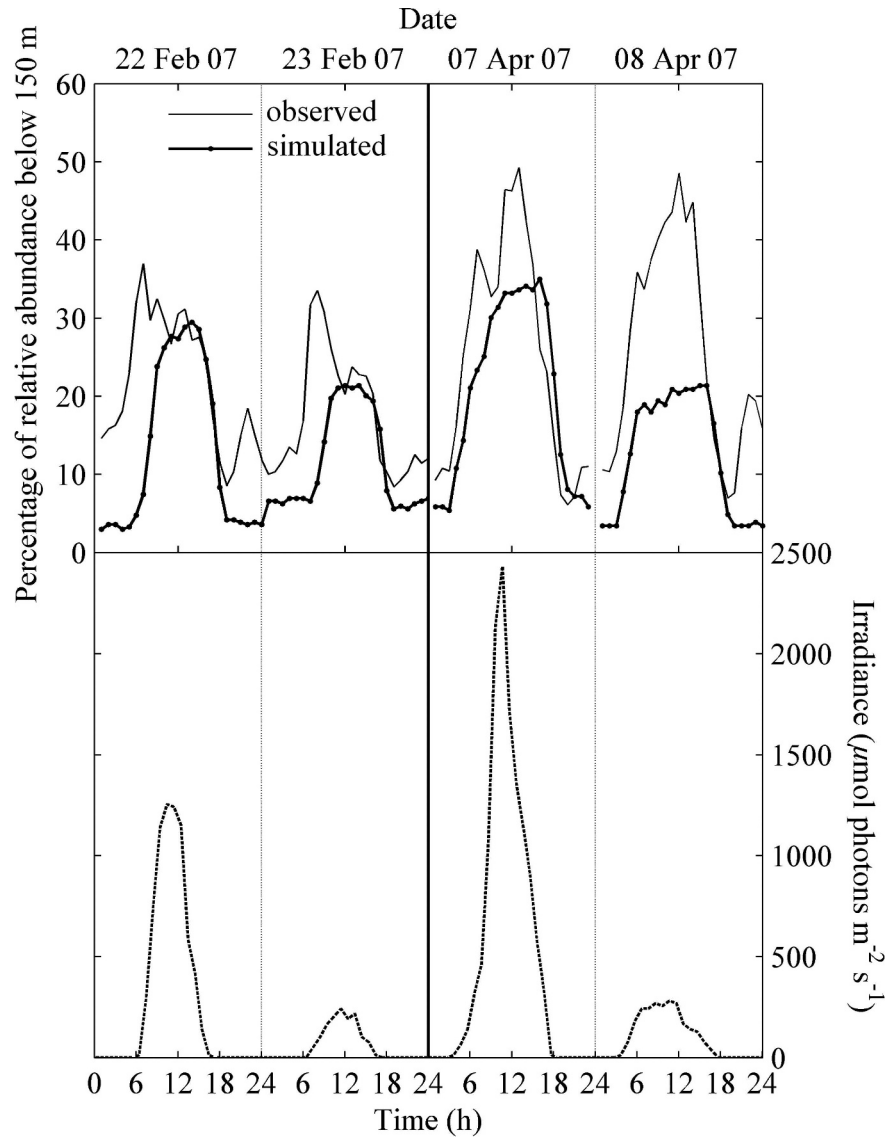


Fig. 9. Simulated and observed relative abundances of *P. periphylla* below 150-m depth in Lurefjorden. The relative abundance is given as a percentage of the maximal abundance observed (thin line) or simulated (bold line) for the water column. Surface irradiance is indicated in the lower panel.

In the simulations, we assumed constant light during night, and in this situation extensive vertical individual night excursions can be simulated only according to the likelihood that an individual remains migrating in the same direction for a large time period. The random walk-based probability that an individual should migrate 200 m up and down in the water column during an 18-h night equals  $4.2 \times 10^{-146}$ . Assuming a total population of  $10^{10}$  *P. periphylla* in Lurefjorden (which is most likely an overestimate), the probability that one would make this type of migration would be  $4.2 \times 10^{-136}$ , which clearly indicates that our simulations cannot account for the individual night excursions performed by some individuals (Kaaertvedt et al. 2007). In lack of measurements, the assumption of constant light at night therefore prohibits

simulation of such excursions. Values of moonlight range from 0.0001 (Kampa 1970) to  $0.023 \mu\text{mol photons m}^{-2} \text{s}^{-1}$  (Gliwicz 1986), and no moon conditions and cloudiness will obviously increase the range of variation. It is therefore unclear what the simulations would have looked like if actual light measurements at night had been available.

At dawn the observed population migrated downward before the time indicated by the simulation (Figs. 8, 9). As noted previously, the realism of the simulations is constrained by the lack of light measurements at night because of insufficient sensitivity of the light sensor. *P. periphylla* presumably have a much higher light sensitivity than this sensor, and consequently it is to be expected that the observed individuals react before the simulated individuals at dawn.

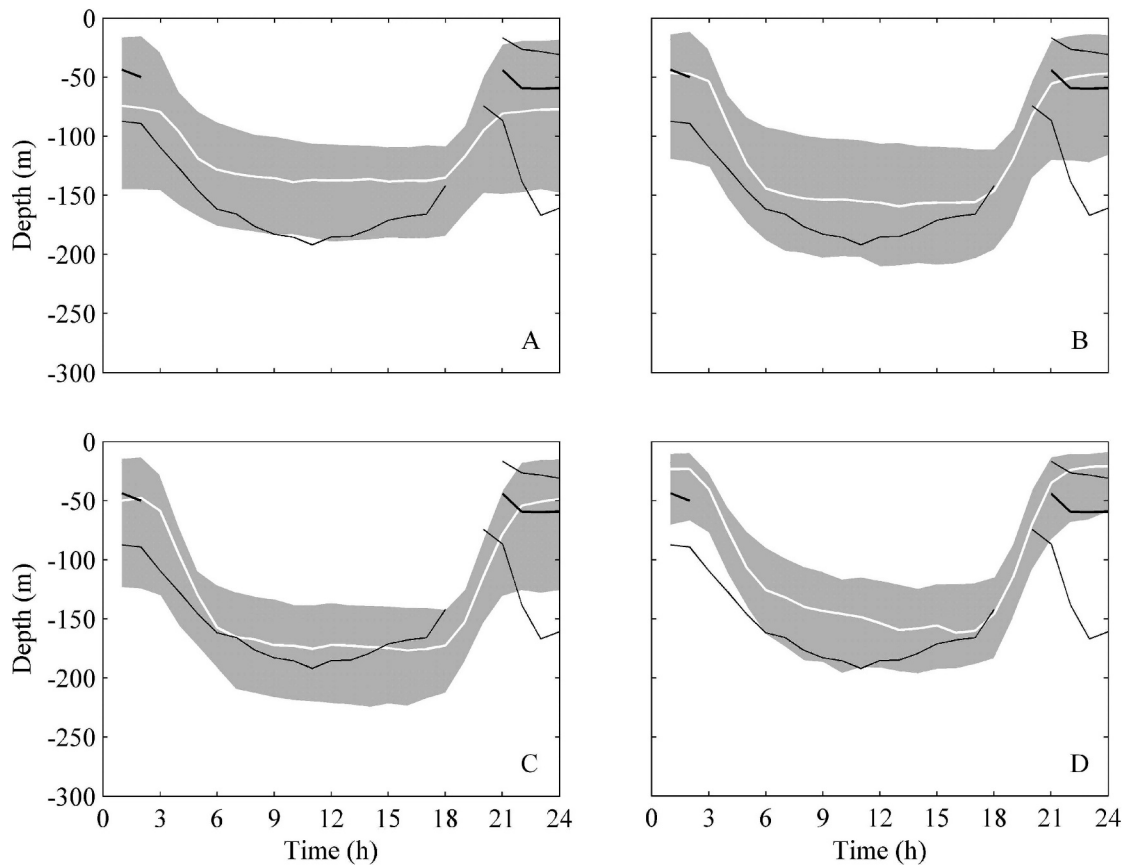


Fig. 10. Simulated (C3) and observed vertical distributions with other parameter values than those used in Figs. 7, 8. (A)  $E_{\min}$  is reduced by 30% relative to the value in Table 3; (B)  $E_{\max}$  is reduced by 30% relative to the value in Table 3; (C)  $K$  is reduced by 25% all over the water column relative to that applied in the simulation in Figs. 7, 8; (D)  $\Delta t$  has been set to 300 s (5 min) relative to the value in Table 3. The observations represent 15 April 2007 and the simulations were forced with the light measurements at this date. See Fig. 7 for explanation of the shaded area and lines.

Our estimates of  $E_{\max}$  and  $E_{\min}$  were approximated from data in Sørnes et al. (2007) and simplifying assumptions about the light intensity and attenuation of downwelling irradiance,  $K$  (Aksnes et al. in press). These inaccuracies could be responsible for inconsistencies between the observed and simulated 80th percentiles. For example, lower values of  $E_{\min}$  (Fig. 10A),  $E_{\max}$  (Fig. 10B), and  $K$  (Fig. 10C) deepen the location of the simulated 80th percentile, while an increase in these values have the opposite effect (not shown). We have also indicated the effect of increasing the time step ( $\Delta t$ ) of the simulation from 21.6 s to 300 s (Fig. 7B vs. Fig. 10D).

The model suggests that vertical distribution and DVM in zooplankton and other organisms can be described by continuous random walk (i.e., random swimming direction) within a vertical habitat that is characterized by a certain range of light intensities. A prediction from this is that the vertical distribution and the vertical migrations of such organisms should relate inversely to the light attenuation coefficient. For locations where the light attenuation of the water column is different, this could be tested. Specifically, it could be tested whether *P. periphylla* are located shallower and more narrowly in a fjord with high light

attenuation than in a fjord with low attenuation (i.e., Fig. 7B vs. 10C).

Experimental assessment of the light sensitivity of *P. periphylla* is required to improve integration between measurements and modeling in future work. A threshold as low as  $6.3 \times 10^{10}$  photons  $\text{m}^{-2} \text{s}^{-1}$  (which corresponds to  $1.05 \times 10^{-13}$   $\mu\text{mol photons m}^{-2} \text{s}^{-1}$ ) has been reported for escape responses in deep-sea crustaceans (Frank and Widder 1994). Thus, the light response of mesopelagic and deep-water organisms such as *P. periphylla* can presumably take place at light levels much lower than what is commonly considered dark.

Despite several shortcomings, we do believe that our IBM approach has provided insight into the DVM of *P. periphylla* but also into DVM phenomenon in general. In particular, we think that the hypothesis that DVM might occur without changes in individual swimming speed serves as an alternative to those equating migration rate at the population level with the swimming rate at the individual level. Furthermore, the IBM approach also provides a simple mechanism to account for the fact that asynchronous and synchronous migrations occur at the same time. In order to further assess how the DVM phenomenon

relates to light forcing, observations at the individual as well as the population level and accurate light measurements during day and night seem to be required.

#### Acknowledgments

We thank Øyvind Fiksen, Alexis De Robertis, and one anonymous reviewer for valuable comments and suggestions and the European Union (EU) Marie Curie Early Stage Training project METAOCEANS (MEST-CT-2005-019678) for financial support of the first author.

#### References

- AKSNES, D. L., N. DUPONT, A. STABY, Ø. FIKSEN, S. KAARTVEDT, AND J. AURE. in press. Coastal water darkening and implications for mesopelagic regime shifts in Norwegian fjords. *Mar. Ecol. Prog. Ser.*
- ALLEN, J. I., P. J. SOMERFIELD, AND F. J. GILBERT. 2007. Quantifying uncertainty in high-resolution coupled hydrodynamic-ecosystem models. *J. Mar. Syst.* **64**: 3–14.
- ANDERSEN, V., AND P. NIVAL. 1991. A model of the diel vertical migration of zooplankton based on euphausiids. *J. Mar. Res.* **49**: 153–175.
- BALK, H., AND T. LINDEM. 2005. Sonar4 and sonar5-pro post processing systems. Operation manual. Lindem Data Acquisition.
- BÅMSTEDT, U., S. KAARTVEDT, AND M. J. YOUNGBLUTH. 2003. An evaluation of acoustic and video methods to estimate the abundance and vertical distribution of jellyfish. *J. Plankton Res.* **25**: 1307–1318.
- CONTOR, C. R., AND J. S. GRIFFITH. 1995. Nocturnal emergence of juvenile rainbow trout from winter concealment relative to light intensity. *Hydrobiologia* **299**: 179–183.
- DAWIDOWICZ, P., AND L. J. CARSTEN. 1992. Metabolic costs during predator-induced diel vertical migration of *Daphnia*. *Limnol. Oceanogr.* **37**: 1589–1595.
- DE ROBERTIS, A. 2002. Size-dependent visual predation risk and the timing of vertical migration: An optimization model. *Limnol. Oceanogr.* **47**: 925–933.
- FIKSEN, Ø., AND F. CARLOTTI. 1998. A model of optimal life history and diel vertical migration in *Calanus finmarchicus*. *Sarsia* **83**: 129–147.
- , C. JØRGENSEN, T. KRISTIANSEN, F. VIKEBØ, AND G. HUSE. 2007. Linking behavioural ecology and oceanography: Larval behaviour determines growth, mortality and dispersal. *Mar. Ecol. Prog. Ser.* **347**: 195–205.
- FOSSÅ, J. H. 1992. Mass occurrence of *Periphylla periphylla* (Scyphozoa, Coronatae) in a Norwegian fjord. *Sarsia* **77**: 237–251.
- FRANK, T. M., AND E. A. WIDDER. 1994. Comparative study of behavioral-sensitivity thresholds to near-UV and blue-green light in deep-sea crustaceans. *Mar. Biol.* **121**: 229–235.
- GISKE, J., G. HUSE, AND Ø. FIKSEN. 1998. Modelling spatial dynamics of fish. *Rev. Fish Biol. Fish.* **8**: 57–91.
- GLIWICZ, Z. M. 1986. A lunar cycle in zooplankton. *Ecology* **67**: 883–897.
- IRIGOIEN, X., D. V. P. CONWAY, AND R. P. HARRIS. 2004. Flexible diel vertical migration behaviour of zooplankton in the Irish Sea. *Mar. Ecol. Prog. Ser.* **267**: 85–97.
- JARMS, G., U. BÅMSTEDT, H. TIEMANN, M. B. MARTINUSSEN, AND J. H. FOSSÅ. 1999. The holopelagic life cycle of the deep-sea medusa *Periphylla periphylla* (Scyphozoa, Coronatae). *Sarsia* **84**: 55–65.
- , G. H. TIEMANN, AND U. BÅMSTEDT. 2002. Development and biology of *Periphylla periphylla* (Scyphozoa: Coronatae) in a Norwegian fjord. *Mar. Biol.* **141**: 647–657.
- KAARTVEDT, S., T. A. KLEVJER, T. TORGERSEN, T. A. SØRNES, AND A. RØSTAD. 2007. Diel vertical migration of individual jellyfish (*Periphylla periphylla*). *Limnol. Oceanogr.* **52**: 975–983.
- KAMPA, E. M. 1970. Underwater daylight and moonlight measurements in the eastern north Atlantic. *J. Mar. Biol. Assoc. U.K.* **50**: 397–420.
- LAMPERT, W., AND U. SOMMER. 2007. *Limnoecology: The ecology of lakes and streams*, 2nd ed. Oxford University Press.
- MANGEL, M., AND C. W. CLARK. 1988. *Dynamic modelling in behavioral ecology*. Princeton University Press.
- PEARRE, S. J. 2003. Eat and run? The hunger/satiation hypothesis in vertical migration: History, evidence and consequences. *Biol. Rev.* **78**: 1–79.
- RICHARDS, S. A., H. P. POSSINGHAM, AND J. NOYE. 1996. Diel vertical migration: Modelling light-mediated mechanisms. *J. Plankton Res.* **18**: 2199–2222.
- RINGELBERG, J. 1999. The photobehaviour of *Daphnia* spp. as a model to explain diel vertical migration in zooplankton. *Biol. Rev.* **74**: 397–423.
- , AND E. VAN GOOL. 2003. On the combined analysis of proximate and ultimate aspects in diel vertical migration (DVM) research. *Hydrobiologia* **491**: 85–90.
- ROSSBERG, M., AND S. A. WICKHAM. 2008. Ciliate vertical distribution and diel vertical migration in a eutrophic lake. *Fundam. Appl. Limnol. (Arch. Hydrobiol.)* **171**: 1–14.
- SØRNES, T. A., D. L. AKSNES, U. BÅMSTEDT, AND M. J. YOUNGBLUTH. 2007. Causes for mass occurrences of the jellyfish *Periphylla periphylla*: A hypothesis that involves optically conditioned retention. *J. Plankton Res.* **29**: 157–167.
- , A. HOSIA, U. BÅMSTEDT, AND D. L. AKSNES. 2008. Swimming and feeding in *Periphylla periphylla* (Scyphozoa, Coronatae). *Mar. Biol.* **153**: 653–659.
- SÖTJE, I., H. TIEMANN, AND U. BÅMSTEDT. 2007. Trophic ecology and the related functional morphology of the deep-water medusa *Periphylla periphylla* (Scyphozoa, Coronata). *Mar. Biol.* **150**: 329–343.
- VALIELA, I. 1995. *Marine ecological processes*. Springer-Verlag.
- YOUNGBLUTH, M. J., AND U. BÅMSTEDT. 2001. Distribution, abundance, behavior and metabolism of *Periphylla periphylla*, a mesopelagic coronate medusa in a Norwegian fjord. *Hydrobiologia* **451**: 321–333.

Associate editor: Thomas Kiorboe

Received: 22 December 2008

Accepted: 12 May 2009

Amended: 02 June 2009